Ligand-elaboration as a strategy for engendering structural diversity in porous metal–organic framework compounds†

Tendai Gadzikwa, Bi-Shun Zeng, Joseph T. Hupp* and SonBinh T. Nguyen*

Received (in Berkeley, CA, USA) 13th September 2007, Accepted 24th April 2008
First published as an Advance Article on the web 30th June 2008
DOI: 10.1039/b714160b

A series of 4,4′-ethynylenedibenzoic acids were synthesized and used in the construction of Zn-based, mixed-ligand metal–organic frameworks; through variation of functionality in the 3- and 3′-positions of these linkers, a collection of MOFs with differing connectivities and varying levels of interpenetration was obtained.

The chemistry of metal–organic frameworks (MOFs) has matured to a stage where, together with the exploratory synthesis and characterization of new materials, there is a growing drive towards designing and synthesizing new materials specifically to study the influence of chemical functionality, catenation, and coordination environment on various MOF applications, *e.g.*, gas uptake, separations, and catalysis.[1–4] Investigations of this kind become more precise with an increased ability to hold constant as many variables as possible, while systematically changing only the property under examination.[5–7] The level of network interpenetration in MOFs has been suggested to play a very important role in many sorption and separation applications, due to its direct impact on pore sizes as well as internal surface area and guest-accessible volume.[8,9] As network interpenetration can be strongly influenced by interactions between the struts in neighboring networks, varying the sterics, chemical functionality and van der Waals surface areas of the ligands might allow one to manipulate catenation. Surprisingly, this has not yet been demonstrated to date, although small changes to the substituents on a parent ligand have been shown to affect topology[10,11] and chirality.[12] In this communication, we report a strategy for diversifying MOFs in which minor changes in the organic ligands lead to significant changes in both the connectivities and the levels of catenation in the resulting structures.

We are interested in the use of anisotropic MOF structures, consisting of both dicarboxylate and dipyridyl ligands, for catalysis,[13] separations, and gas storage;[6,14] specifically, to observe how the chemical pore environment affects MOF performance in these applications. Judging that carboxylates are better suited for modification than pyridines, we set out to find a simple and efficient route to chemically diverse, symmetric dicarboxylic acids which would eventually be employed in the synthesis of Zn paddlewheel MOFs.[15–17] Taking guidance from previous work,[5,15] we focused on the synthesis of anisotropic MOFs from bis(aryl carboxylic acid)ethyne and BIPY classes of ligands. MOFs obtained from dipyridyl and dicarboxylic acids incorporate fewer metal centers in the clusters that comprise the MOF vertices and are generally smaller than the analogous Zn_4O clusters found in cubic isoreticular MOFs. Together with the relatively long lengths of the BIPY and bis(aryl carboxylic acid)ethyne struts, the use of slightly smaller clusters should facilitate the interpenetration of up to several independent networks.

We found the one-pot synthesis of bisarylethynes *via* Sonogashira coupling to be invaluable here, as it is reliable, high-yielding, and tolerant to a wide range of functional groups.[18] This last property is particularly useful, as it allows one to efficiently create different functional environments within MOFs possessing similar struts. Additionally, and most notably, we are able to investigate how small changes in ligands, at points remote from their coordinating groups, lead to significant changes in the topologies and levels of interpenetration of the resulting MOFs. To this end, a series of 4,4′-(1,2-ethynediyl)bis(benzoic acid)s (**1a–d**, Fig. 1) was synthesized and applied to the construction of anisotropic MOFs **A–D**. These were formed in good yields upon heating dimethylformamide (DMF) solutions of $Zn(NO_3)_2{\cdot}6H_2O$, the appropriate diacid, and 4,4′-dipyridyl (BIPY) in sealed vials.

We were surprised to obtain the four-fold interpenetrating diamond-like structure **A** (Fig. 2) from **1a**, as several two-fold interpenetrating Zn paddle-wheel MOFs[15] have been synthesized in our labs under the same conditions. Despite having only a single Zn atom complexing two **1a** and two BIPY ligands at the vertex, **A** is remarkably stable. Thermogravimetric analysis (TGA) of a bulk sample of **A** showed that the structure can be desolvated and resolvated reversibly. Additionally, **A** exhibited the same powder X-ray diffraction (PXRD) pattern before and after evacuation (see ESI†).

Ligand **1b**, possessing methyl groups in the 3,3′ position of the dibenzoic acid moiety, gave a three-fold interpenetrating, paddle-wheel MOF structure (**B**, Fig. 3), which, in our experience, is rare

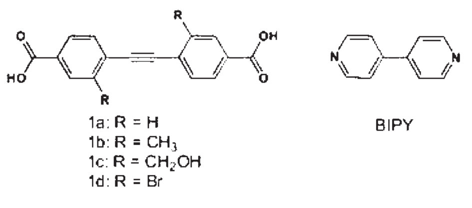

Fig. 1 Ligands used in synthesis of Zn-based mixed-ligand MOFs.

Department of Chemistry and the Institute for Catalysis in Energy Processes, Northwestern University, 2145 Sheridan Road, Evanston, IL 60208-3113, USA. E-mail: j-hupp@northwestern.edu; stn@northwestern.edu; Fax: +1 874-467-1425; +1 874-491-7713; Tel: +1 847-491-3504; +1 847-467-3347

† Electronic supplementary information (ESI) available: Synthetic protocols and characterization data for compounds **1a–d**; TGA and PXRD data for **A–D**; N_2 and H_2 isotherms for **C**; Ar isotherms for **A** and **B**; CIF file for **A**, **B** and **D** and [P4P + RAW] data files for **C**. CCDC 661009–661012. See DOI: 10.1039/b714160b

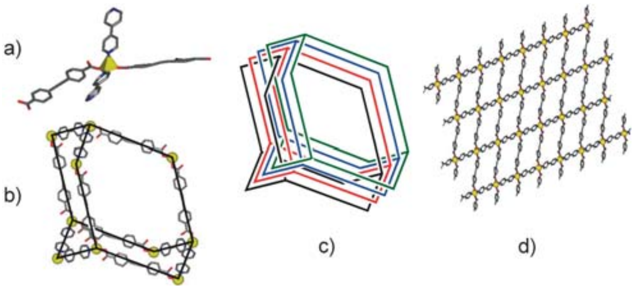

Fig. 2 Views of **A**: (a) Single vertex in the network. The yellow polyhedron represents the zinc ion complexing two **1a** and two BIPY ligands. Carbon: gray; oxygen: red; nitrogen: blue. (b) A schematic representation of the single network unit in **A**. (c) A schematic representation of the four-fold network interpenetration in **A**. (d) A view down the crystallographic *b*-axis of **A**, showing open channels.

for pillared paddlewheel compounds. (Indeed, in our labs we have encountered only one other example.) Despite the relatively high degree of interpenetration, **B** is characterized by a substantial void volume (34%, calculated by PLATON). Upon evacuation and resolvation, it only loses a modest amount of its capacity to take up DMF, as evidenced by TGA experiments (see ESI†). Although this may be due to partial collapse of the pores, PXRD indicates that the resolvated sample retains its crystallinity (see ESI†).

When the steric bulk of the 3,3′-disubstituted bisarylethyne strut was increased by replacing the methyl groups with hydroxymethyls, as in **1c**, we obtained single crystals of material **C**. While the current single-crystal diffraction data were inadequate for modeling all the disorder in the ligands, we are confident that this structure is a two-fold interpenetrating, pillared-paddlewheel framework (Fig. 3, **C**. See Notes and references section for unit cell data).‡

Hypothesizing that differences in steric demand for the bisarylethyne struts were responsible for the differences in interpenetration, we synthesized ligand **1d**, with 3,3′-Br moieties that are similar in size to the methyl groups of **1b**,[19] and combined it with BIPY in MOF synthesis. The resulting structure **D** was indeed three-fold interpenetrating (Fig. 3), like **B**. This result supports the notion that direct influence over the catenation structure of MOFs can be obtained by synthetic manipulation of the sterics of the organic building blocks.

We investigated and compared the gas adsorption capabilities of **A**, **B**, and **D** (Fig. 4; the isotherms of compound **C** were not included as the material is unstable to evacuation (see ESI for XRD and TGA data†)). Surprisingly, **A** adsorbs neither N_2 nor H_2 at 77 K, despite the finding that it can be evacuated and resolvated reversibly with DMF at room temperature (Fig. 4). However, it does adsorb CO_2 at 273 K, giving a Langmuir surface area of 200 $m^2\ g^{-1}$. Most likely, the larger kinetic energy of the CO_2 molecules at higher temperature, together with the greater framework flexibility at 273 K, allows the sorbate to enter pores that are too narrow and rigid at 77 K.[20]

Interestingly, and in contrast to **A**, **B** readily took up both N_2 and H_2, despite indications that its structure may have partially collapsed when desolvated (its TGA data show ~20% loss of DMF uptake capacity, see ESI†). Analysis of the N_2 uptake for **B** based on a type-I Langmuir isotherm yielded a Brunauer–Emmett–Teller (BET) surface area of 650 $m^2\ g^{-1}$. Analysis of the CO_2 isotherm of **B** gave a Langmuir surface area of 400 $m^2\ g^{-1}$ (data were insufficient

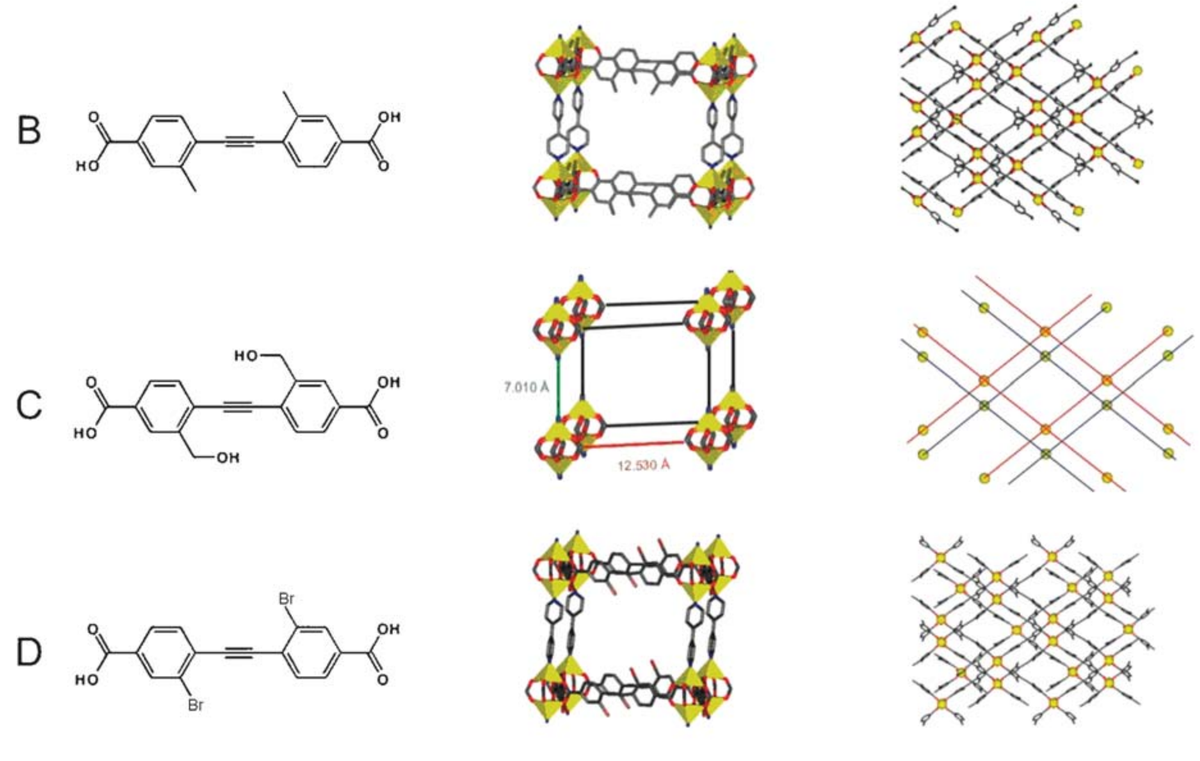

Fig. 3 Paddlewheel MOF structures **B**, **C**, and **D**. Left column: Chemical structures of the corresponding ligands **1b**, **1c**, and **1d**. Center column: Schematic representations of the single network units in each MOF. Right column: Views down BIPY axes showing network interpenetration and framework pores for each MOF. Only the metal-cluster corners for structure **C** are shown as the single-crystal X-ray diffraction data were too weak to establish the location of the ligand atoms with absolute confidence.

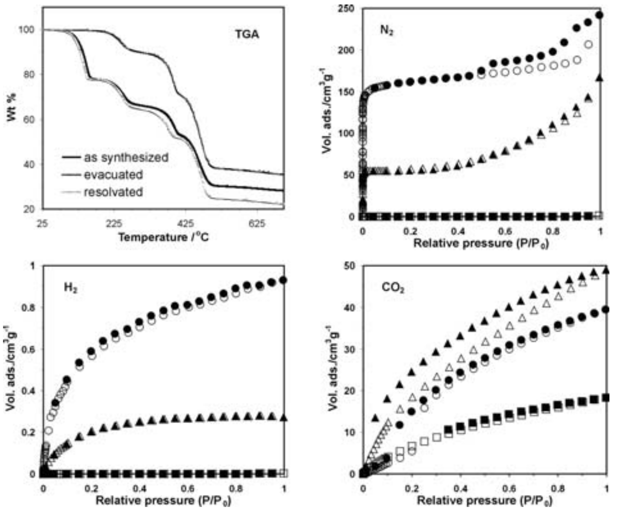

Fig. 4 Top left: TGA curves for **A**. Remaining panels, clockwise from top right: N_2, CO_2, and H_2 adsorption (open), and desorption (closed) isotherms for **A** (□), **B** (○), and **D** (△).

for BET fitting). The difference in adsorption capabilities of the two materials can potentially be attributed to the smaller pore mouth of **A**, ~7 Å *vs.* ~12 Å for **B**. Indeed, when Ar, a probe with a similar kinetic diameter to N_2 (cross-sectional area for Ar is 14.2 Å^2 *vs.* ~16.2 Å^2 for N_2), was used in the gas sorption experiments, the results were similar to those for the N_2 uptake, with only **B** indicating adsorption within the pores. Structure **B** also adsorbed H_2, with an uptake of ~1 wt% at 1 atm and 77 K.

As expected, based on similar ligand sterics and degree of catenation to **B**, **D** also adsorbed all three gases, with H_2 uptake of ~0.3 wt% at 1 atm and 77 K. The BET surface area based on N_2 adsorption was 230 m^2 g^{-1}, while CO_2 gave a Langmuir surface area of 280 m^2 g^{-1}. That only **B** and **D**, among the four materials reported herein, can take up all three gases suggests a "Goldilocks" principle for designing MOFs with good general gas-sorption capabilities: the pores of such MOFs must be large enough to allow gas molecules to access the MOF interior, but not so large as to be non-robust.

In conclusion, we have demonstrated that substituents in ligand struts can be used as structure-influencing tools in the synthesis of MOFs with different levels of catenation. That small changes in the side groups of the ethynylene dibenzoate struts, from H to Me and CH_2OH, can lead to three different structures, all with large pores and different gas adsorption behaviors, hints at the vast potential for manipulating solid structures *via* organic synthesis. In addition, because similarly sized Me and Br substituents afford similarly interpenetrated MOFs, it may be possible that ligand sterics can be relied on to induce specific topologies with different chemical environments.

While the results described herein pertain to a specific set of ligands and metal ion, there exists a tantalizing possibility that a wide range of different MOF structures can be accessed with very nearly the same ligand motif. By modifying the substituents of the organic struts, a diverse collection of MOFs with differing connectivities and varying levels of interpenetration should be possible, allowing one to unravel the effect of chemical functionality and structural differences on the material properties of MOFs.

We acknowledge the Institute of Catalysis for Energy Processes at Northwestern University, AFOSR, NSF, and the Basic Energy Sciences Program, Office of Science, US Department of Energy (Grant No. DE-FG02-01ER15244) for support of this work.

Notes and references

‡ Crystal data. Compound **A**: $C_{32}H_{30}N_4O_6Zn_1$, M = 631.97, monoclinic, $C2/c$, a = 28.848(7), b = 6.1751(15), c = 17.144(4) Å, β = 98.838(4)°, U = 3017.8(13) Å^3, Z = 4, D_c = 1.391 g cm^{-3}, μ = 0.850 mm^{-1}, F(000) = 1312, GOF = 1.111. $R1$ and w$R2$ are 0.072 and 0.195, respectively for 197 parameters and 2702 reflections [$I > 2\sigma(I)$]. Compound **B**: $C_{69}H_{48}N_3O_{12}Zn_{13}$, M = 1307.21, monoclinic, $C2$, a = 21.792(2), b = 27.979(3), c = 14.0334(15) Å, β = 93.579(2)°, U = 8539.9(16) Å^3, Z = 4, D_c = 1.017 g cm^{-3}, μ = 0.88 mm^{-1}, F(000) = 2676, GOF = 0.89. $R1$ and w$R2$ are 0.051 and 0.116, respectively for 783 parameters and 11 758 reflections [$I > 2\sigma(I)$]. Compound **C**: $C_{46}H_{32}N_2O_{12}Zn_2$, M = 935.52, monoclinic, $C2$, a = 21.909(16), b = 27.458(16), c = 14.013(9) Å, β = 93.183(17)°, U = 8417(10) Å^3. Compound **D**: $C_{126}H_{60}Br_{12}N_6O_{24}Zn_6$, M = 3392.94, monoclinic, $P2(1)$, a = 14.0828(9), b = 28.2518(18), c = 21.4518(14) Å, β = 93.5600(10)°, U = 8518.4(9) Å^3, Z = 2, D_c = 1.323 g cm^{-3}, μ = 3.70 mm^{-1}, F(000) = 3300, GOF = 0.91. $R1$ and w$R2$ are 0.066 and 0.199, respectively for 1565 parameters and 22 525 reflections [$I > 2\sigma(I)$]. The data were collected on a SMART CCD 1000 with MoKα radiation (i) 0.710 73 Å at 120 K. The structures were solved by direct methods and refined by a full matrix least-squares technique based on $F2$ using the SHELXL 97 program. Modeling of solvent molecules for all but **A** proved impossible due to severe disorder, thus the SQUEEZE subroutine in the PLATON software package was applied to mask the electron density in the cavities. CCDC 661009–661012.

1 C.-J. Li, S. Hu, W. Li, C.-K. Lam, Y.-Z. Zheng and M.-L. Tong, *Eur. J. Inorg. Chem.*, 2006, 1931–1935.
2 J. L. C. Rowsell and O. M. Yaghi, *J. Am. Chem. Soc.*, 2006, **128**, 1304–1315.
3 R. Vaidhyanathan, D. Bradshaw, J.-N. Rebilly, J. P. Barrio, J. A. Gould, N. G. Berry and M. J. Rosseinsky, *Angew. Chem., Int. Ed.*, 2006, **45**, 6495–6499.
4 A. G. Wong-Foy, A. J. Matzger and O. M. Yaghi, *J. Am. Chem. Soc.*, 2006, **128**, 3494–3495.
5 M. Eddaoudi, J. Kim, N. Rosi, D. Vodak, J. Wachter, M. O'Keeffe and M. Yaghi Omar, *Science*, 2002, **295**, 469–472.
6 B. Chen, S. Ma, F. Zapata, E. B. Lobkovsky and J. Yang, *Inorg. Chem.*, 2006, **45**, 5718–5720.
7 X. Lin, J. Jia, X. Zhao, K. M. Thomas, A. J. Blake, G. S. Walker, N. R. Champness, P. Hubberstey and M. Schroeder, *Angew. Chem., Int. Ed.*, 2006, **45**, 7358–7364.
8 B. Kesanli, Y. Cui, R. Smith Milton, W. Bittner Edward, C. Bockrath Bradley and W. Lin, *Angew. Chem., Int. Ed.*, 2004, **44**, 72–75.
9 J. L. C. Rowsell and O. M. Yaghi, *Angew. Chem., Int. Ed.*, 2005, **44**, 4670–4679.
10 X.-C. Huang, Y.-Y. Lin, J.-P. Zhang and X.-M. Chen, *Angew. Chem., Int. Ed.*, 2006, **45**, 1557–1559.
11 A. L. Grzesiak, F. J. Uribe, N. W. Ockwig, O. M. Yaghi and A. J. Matzger, *Angew. Chem., Int. Ed.*, 2006, **45**, 2553–2556.
12 D. Bradshaw, T. J. Prior, E. J. Cussen, J. B. Claridge and M. J. Rosseinsky, *J. Am. Chem. Soc.*, 2004, **126**, 6106–6114.
13 S.-H. Cho, B. Ma, S. T. Nguyen, J. T. Hupp and T. E. Albrecht-Schmitt, *Chem. Commun.*, 2006, 2563–2565.
14 H. Chun, D. N. Dybtsev, H. Kim and K. Kim, *Chem.–Eur. J.*, 2005, **11**, 3521–3529.
15 B.-Q. Ma, K. L. Mulfort and J. T. Hupp, *Inorg. Chem.*, 2005, **44**, 4912–4914.
16 D. N. Dybtsev, H. Chun and K. Kim, *Angew. Chem., Int. Ed.*, 2004, **43**, 5033–5036.
17 S. I. Vagin, A. K. Ott and B. Rieger, *Chem.-Ing.-Tech.*, 2007, **79**, 767–780.
18 M. J. Mio, L. C. Kopel, J. B. Braun, T. L. Gadzikwa, K. L. Hull, R. G. Brisbois, C. J. Markworth and P. A. Grieco, *Org. Lett.*, 2002, **4**, 3199–3202.
19 L. Pauling, *The Nature of the Chemical Bond*, Cornell University Press, New York, 3rd edn, 1960.
20 D. Cazorla-Amoros, J. Alcaniz-Monge and A. Linares-Solano, *Langmuir*, 1996, **12**, 2820–2824.